

Article

# Assessing Boundary Film Forming Behavior of Phosphonium Ionic Liquids as Engine Lubricant Additives

Mayank Anand<sup>1,2,\*</sup>, Mark Hadfield<sup>1</sup>, Jose-Luis Viesca<sup>1,2</sup>, Ben Thomas<sup>1</sup>, Ruben González<sup>1,3</sup>, Rob Cantrill<sup>4</sup> and Antolin Hernández Battez<sup>1,2</sup>

<sup>1</sup> Department of Design and Engineering, Bournemouth University, Poole BH12 5BB, UK; mhadfield@bournemouth.ac.uk (M.H.); viescajose@uniovi.es (J.-L.V.); thomasb@bournemouth.ac.uk (B.T.); gonzalezruben@uniovi.es (R.G.); aehernandez@uniovi.es (A.H.B.)

<sup>2</sup> Department of Construction and Manufacturing Engineering, University of Oviedo, 33203 Gijón, Asturias, Spain

<sup>3</sup> Department of Marine Science and Technology, University of Oviedo, 33203 Gijón, Asturias, Spain

<sup>4</sup> Royal National Lifeboat Institution, Headquarter, Poole, BH15 1HZ, UK; Rob\_Cantrill@rnli.org.uk

\* Correspondence: m.anand8@yahoo.com; Tel.: +44-7438259072

Academic Editor: James E. Krzanowski

Received: 18 February 2016; Accepted: 10 May 2016; Published: 30 May 2016

**Abstract:** The reduction of friction and wear losses in boundary lubrication regime of a piston ring-cylinder liner tribo-system has always been a challenge for engine and lubricant manufacturers. One way is to use lubricant additives, which can form boundary film quickly and reduce the direct contact between asperities. This article focuses on the assessment of boundary film forming behavior of two phosphonium-based ionic liquids (ILs) as additives in engine-aged lubricant to further improve its film forming capabilities and hence reduce friction and wear of contacting surfaces. A reciprocating piston ring segment-on-flat coupon under fully flooded lubrication conditions at room temperature (approx. 25 °C) was employed. The trihexyltetradecyl phosphonium bis(2-ethylhexyl) phosphate and trihexyltetradecyl phosphonium bis(2,4,4-tri-methylpentyl) phosphinate ionic liquids were used as additives in 6 vol. % quantity. Benchmark tests were conducted using fully formulated new lubricant of same grade (with and without ILs). Results revealed that the addition of phosphonium ILs to engine-aged lubricant led to quicker initiation of boundary film forming process. In addition, friction and wear performance of engine-aged lubricant improved by the addition of both ILs and these mixtures outperformed the fresh fully formulated oil. Chemical analysis showed higher concentration of phosphorus element on the worn surface indicating presence of ILs in the formed tribofilms.

**Keywords:** phosphonium ionic liquids; additives; friction; wear; boundary film formation

## 1. Introduction

Improved fuel economy and lower emissions demand for higher energy-conserving engine oils and better fuel-efficient vehicles [1]. Different engine components may experience different and/or more than one lubrication regime during operation [1]. Notably, 40%–50% of total frictional loss accounts to the sliding contact of piston rings against the cylinder liner surface alone [1,2]. The larger part of the cylinder liner—the piston ring interaction area during each piston stroke—experiences Elasto-Hydrodynamic Lubrication (EHL). Thus, frictional losses in this region are attributed to traction produced by shearing of pressurized lubricant film at the contact interface. The use of low viscosity lubricants can result in low viscous shear and hence less frictional losses can be achieved [3]. However, this could increase the boundary frictional losses and wear resulting from increased asperities

interactions. Therefore, current developments are focused on enhancing the performance of lubricants in the boundary-lubricated regime.

In a ring-liner tribo-system near top dead center (TDC) region, the surface properties and the chemical composition of the lubricant are significant. The momentary cessation of lubricant entrainment in ring-liner contact results in an asperities interaction since the lubricant is retained in the contact zone due to either squeeze film action or entrapment in the rough contiguous surfaces [4,5]. Due to high mechanical and thermal stresses experienced by the lubricant in this region, its additive content chemically reacts with either sliding surface to form protective layers covering the asperities. Such layers are formed by the polar molecules of the additives, which generally possess a long chain structure with an inherent lower shear strength than the underlying solid surface, thus separating the surfaces and reducing wear and frictional losses.

Since 2001, many studies have reported on the tribological properties of ionic liquids (ILs) as an additive in mineral and/or synthetic base oils [3,6–10], and others on their use as engine lubricants [3,4,7,11,12]. ILs have some key inherent properties that make them suitable for an engine environment, such as high thermal stability, very low volatility, non-flammability, detergency in being a solvent, they are non-corrosive, have good wettability, and excellent tribological performances [3,7]. In this article, the authors present their recent experimental work on the assessment of boundary film forming behavior of two phosphonium-based ILs as additives in an engine-aged lubricant. The performance was benchmarked against the fully formulated new lubricant of the same grade.

## 2. Materials and Methods

### 2.1. Lubricants

The ionic liquids, IL1 and IL2, used in this work are described in Table 1. These ILs were added (separately) as 6 vol. % concentrations to a commercially available fully-formulated mineral-based SAE 15W40. Engine-aged lubricant samples (Used Oil) were collected from the diesel engine (MAN D2840LE401, heavy duty 4-stroke, power output ~850 hp) used in Trent Class Lifeboats of the Royal National Lifeboat Institution (RNLI) in the United Kingdom. These oil samples were collected after 315 h of engine servicing. For reference purposes, fresh oil (New Oil) samples of same grade, with and without ILs, were also tribologically tested. The viscosities of the engine oils were experimentally measured according to ASTM D445. An ultrasonic probe was used for 5 min to mix the oil and IL samples. No phase separation between New Oil and IL was observed by visual inspection, even a month after the mixing process. The stability of the mixtures of Used Oil and IL was measured by a light backscattering technique, as explained in Section 3. In addition, since one of the objectives of this study is to assess the feasibility of using ILs in the way that they are commercially available (impurities included), the as-supplied version of ILs were used in the experiments without any further purification.

**Table 1.** Details of phosphonium ionic liquids (ILs) used in tribological testing.

Additive/Lubricant	Description	Purity (%)	Density (g/mL)			Viscosity (cSt)		
			23 °C	40 °C	100 °C	23 °C	40 °C	100 °C
IL1 *	Trihexyltetradecyl phosphonium bis(2,4,4-tri-methylpentyl) phosphinate	>95	0.90	388.8	35.4			
IL2 *	Trihexyltetradecyl phosphonium bis(2-ethylhexyl) phosphate	>98	0.91	429.0	49.5			
New Oil ‡	Fresh SAE 15W40	-	0.886	106.1	14.3			
Used Oil ‡	Engine-aged SAE 15W40	-	0.884	91.5	12.7			

Source of information: \* Reference [9]; ‡ [6].

## 2.2. Test Set-Up and Experimental Conditions

Tribological tests were conducted using a High Frequency reciprocating tribometer (Plint TE77). Figure 1 shows the schematic of the test configuration using a piston ring segment and a flat coupon under lubricated conditions. Table 2 shows the test conditions used for each tribo-test. Contact pressure was calculated using the Hertz theory for non-conformal contacts, as mentioned in Reference [13]. Electrical contact resistance (ECR) was measured to understand the boundary film formation process using the Lunn-Furey ECR Circuit [14]. Each test was repeated three times and mean of friction coefficient and wear volume data were reported.

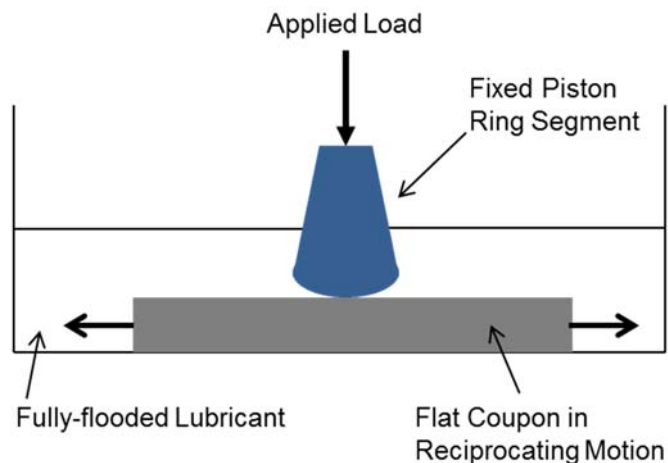


Figure 1. Schematic of test set-up used in the current study.

Table 2. Test conditions.

Test Parameter	Value	Unit
Contact Pressure	285	MPa
Applied Load	50	N
Sliding Frequency	4.4	Hz
Stroke Length	5	mm
Oil Temperature	25	°C
Test Duration	3	h

The specimens used in the tribological tests were prepared to simulate the piston ring-cylinder liner contact. Top compression piston rings utilized in MAN D2840LE401 engines were cut into several small segments (length = 24 mm) to be used as the upper specimen. Flat coupons (W 10 mm × L 33 mm) with a similar material composition (grey cast iron BS1452) to that of the actual cylinder liners used in the same engine were employed as the lower specimen. A simplified non-conformal configuration was employed instead of conformal contacting surfaces in order to avoid misalignment issues. Before tribological tests, both the upper and lower specimens were cleaned in an ultrasonic bath with acetone for 10 min. Table 3 shows the chemical compositions of the flat coupons and the piston ring coating on its running face.

**Table 3.** Material description of test samples.

Test Sample	Fe (%)	C (%)	Si (%)	Mn (%)	P (%)	S (%)	Cr (%)	O (%)
Flat coupon <sup>1</sup>	Rem.	3.0–3.3	2.4–2.6	0.7–1.0	0.4–1.1	0.1–1.1	-	-
Piston ring (coating) <sup>2</sup>	-	4.92	-	-	-	-	93.53	1.55

Source of information: <sup>1</sup> Supplier; <sup>2</sup> Energy Dispersive X-ray (EDX) analysis of piston ring coating cross-section.

### 2.3. Surface Analysis

The wear scars on the flat coupons were analyzed after each tribological test. Wear volume was measured using a 3D White Light Interferometer (ZYGO Corporation, Middlefield, CT, USA). Scanning Electron Microscopy (SEM) manufactured by JEOL Ltd., Tokyo, Japan (Model JSM-6610LV) was used to study the wear mechanisms. Energy Dispersive X-ray (EDX, Inca Energy-350, Oxford Instruments, Oxfordshire, UK) and X-ray Photoelectron Spectroscopy (XPS, SPECS, Berlin, Germany) performed the chemical analysis of wear scars. The XPS analysis was performed using a SPECS Phoibos 100 MCD5 system equipped with a hemispherical electron analyzer, and the spectra were analyzed using CasaXPS software (Casa Software Ltd.). Further details of the equipment used can be found in the previous work of the authors [6].

## 3. Results and Discussion

### 3.1. Oil-IL Mixture Stability Analysis

The stability of mixtures containing non-polar engine oil and polar ILs is very important for overall performance, both during the testing stage and in real applications. Using ILs as an additive in fully formulated lubricants can be a challenge since it may lead to an unstable emulsion. Yu *et al.* [9] demonstrated the verification of oil stability by using the comparison of the experimentally measured viscosity of the oil-IL mixture with the theoretical viscosity value obtained by the Refutas equation. In the current research, an optical scanning technique using Turbiscan Lab Expert (manufactured by Formulacion, L'Union, France) was employed for analyzing oil stability. This technique has been employed in the past for analyzing the dispersion and suspension state of various oils and mixtures containing ILs [15–23]. Four different mixtures of IL1 and IL2 with New Oil and Used Oil were analyzed; only the results for Used Oil are discussed in this paper.

Since Used Oil is slightly less dense (0.884 g/mL) than both ILs (~0.91 g/mL), the density difference can result in sedimentation of the heavier dispersed phase (IL) in the less dense continuous phase (Used Oil). The presence of wear debris in the engine-aged (Used Oil) sample can also lead to sedimentation processes. Such phenomena may result in a change of transmission and/or backscattering of light through the sample where the concentration of the dispersed phase changes over time.

Figure 2 shows the stability analysis spectra, for the mixtures of IL1 and IL2 with Used Oil, collected over a period of 11 days. Clearly, these mixtures can be considered as stable and single phase homogeneous. Similar results were noted for the blends of ILs with New Oil. Plausible reasons for the lack of sedimentation of wear debris could be attributed to the presence of remaining dispersant additives in the fully formulated Used Oil. Dispersant additives are responsible for keeping all contaminants dispersed in the oil during engine operation so that debris can be filtered out when the oil is passed through the oil filter instead of depositing over the surface of lubricated engine components.

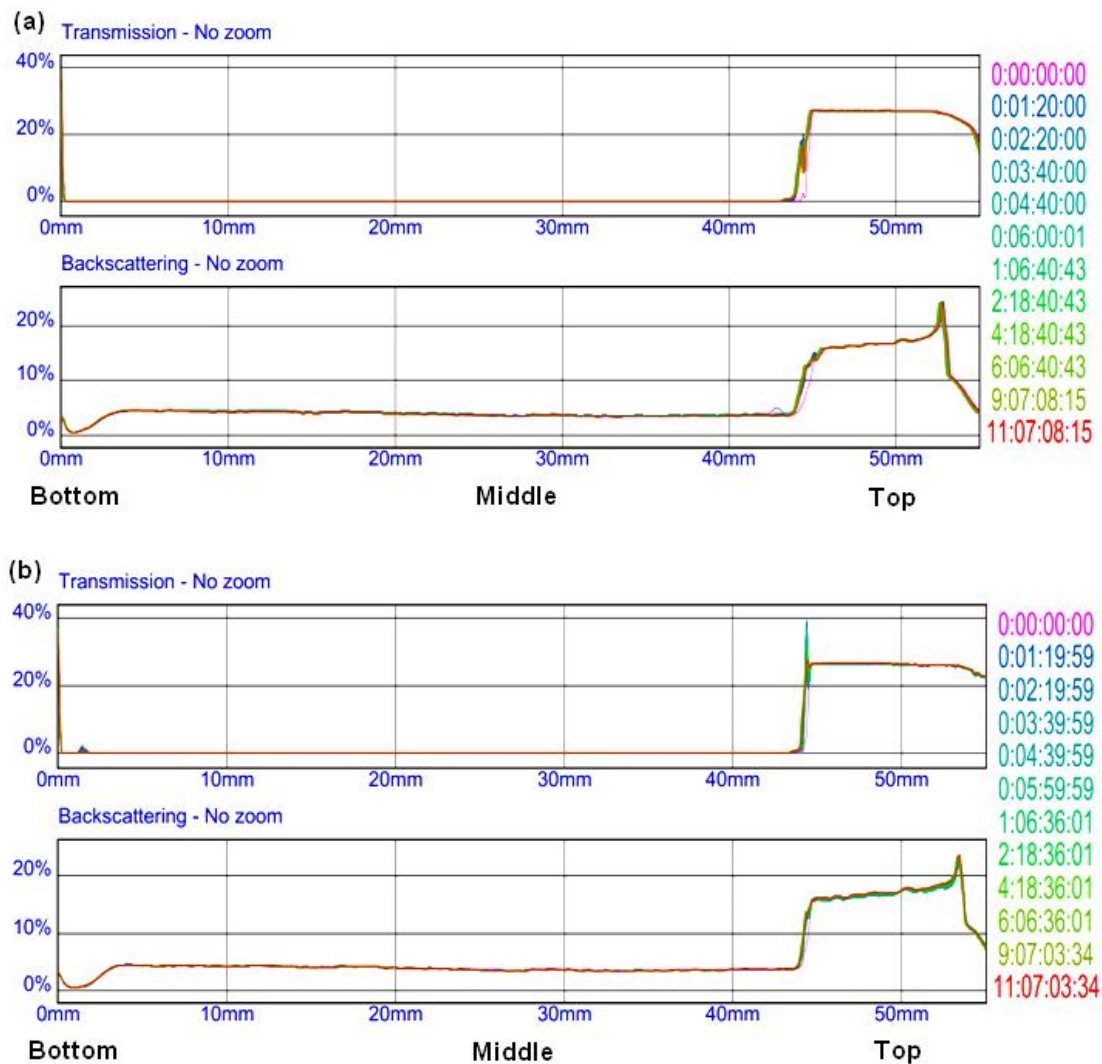


**Figure 2.** Stability analysis spectra of 6% IL1 (a); and 6% IL2 (b) in Used Oil. The horizontal axis corresponds to height of oil sample (45 mm) in bottle and color of different profiles corresponds to time scale (day:h:min:s) on vertical axis on the right.

### 3.2. Friction and Film Forming (ECR) Behavior

Friction coefficient values ( $\sim 0.1$ ) indicate the boundary lubrication regime during the tribo-testing (Figure 3). Fast-transition in the friction coefficient ( $>0.2$ ), which is representative of increased adhesion between sliding surfaces leading to scuffing failure, was not observed in any case.

A quantitative comparison of boundary film formation behavior of oils, with and without ILs, was made using ECR curves based on the theory proposed by Yamaguchi *et al.* [24]. According to their theory, at the beginning of sliding, chemical changes may be occurring that result in surface species beginning to form, and, with continued sliding, a sufficient accumulation of such species results in rapid boundary film formation. The time interval between the start of sliding and the start of film formation is defined as the induction time. A clear difference in the induction time after the addition of ILs to the New and Used Oil can be seen in the ECR results shown in Figure 4.

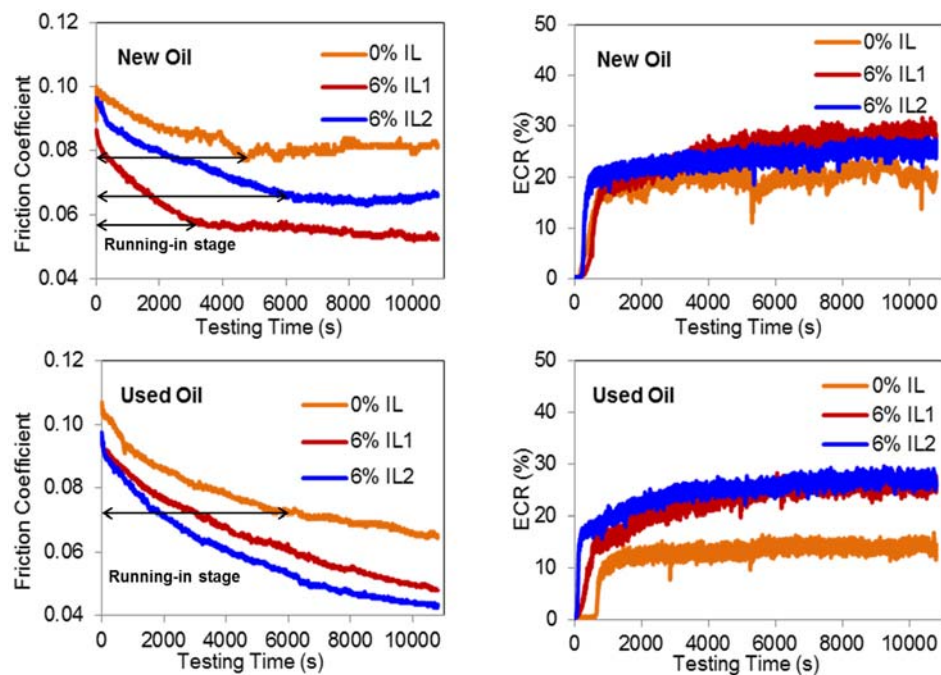


**Figure 3.** Mean Friction Coefficient and representative electrical contact resistance (ECR) results for testing time of 3 h.

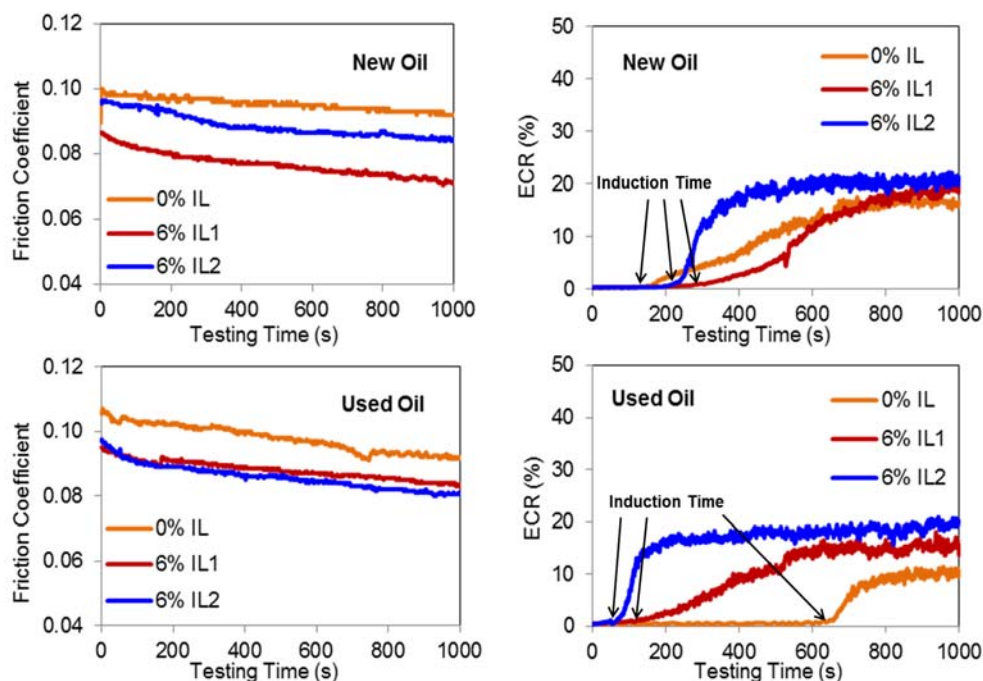


**Figure 4.** Mean Friction Coefficient and representative ECR results for testing time of the initial 1000 s.

The friction–time curve, in Figure 3, shows that the running-in stage for New Oil lasted for approx. 5000 s. After the addition of ILs, the running in stage reduced to approx. 3000 s for IL1 and increased to approx. 6000 s for IL2. Clearly, the overall friction performance of New Oil with IL1 was better than with IL2 during both the running in and the steady state sliding periods. ECR curves in Figure 3 suggest the formation of a slightly thicker boundary film in the case of IL1 as opposed to IL2, followed by pure New Oil, which could be the reason for the better friction response of IL1. To further

understand the film formation behavior of different oil mixtures, a closer look at the friction and ECR curves was made by considering only the initial 1000 s of the sliding test. Figure 4 demonstrates an increase in the induction time for New Oil from 169 to 309 and 222 s by the addition of IL1 and IL2, respectively. Additionally, the time to reach a stable boundary film for New Oil has also increased considerably, from 680 s to 1000 s, by the addition of IL1, and, was reduced to 422 s by the addition of IL2. The results suggest that addition of both ILs slightly delayed the induction time, but that IL2 was able to form a stable film much quicker than IL1, which responded gradually and was similar to pure New Oil.

In the case of Used Oil, in Figure 3, the steady-state friction was reached at 6200 s, but was only short-lived until 9000 s, after which time the friction coefficient dropped again. Addition of both ILs improved the friction performance of Used Oil, but showed no distinction in the overall trend. The friction coefficient dropped continuously in a quasi-linear manner from the beginning of tribo-test. This phenomenon was ascribed to the fact that various processes begin to operate during the running-in stage. The superposition of their influence leads to complex frictional changes until a balance (or equilibrium) is achieved, but sometimes these processes continue to evolve and steady-state is either not achieved or short-lived [25]. Unlike New Oil, IL2 additive showed lower friction and formed a thicker film than IL1 in Used Oil. Furthermore, Figure 4 shows that, after the addition of ILs, the induction time for Used Oil was reduced from 646 to 100 and 64 s for IL1 and IL2, respectively. Additionally, the time to reach stable boundary film for Used Oil also reduced from 755 to 550 and 150 s by addition of IL1, and IL2, respectively. These results clearly showed that the boundary film formation process initiated much earlier in case of IL2 than IL1, followed by pure Used Oil.

These observations suggest that film-forming behavior of both ILs are distinct from each other. IL2 is capable of initiating the boundary film formation process leading to a stable film quicker than IL1. However, potentially, depending on the quality of base lubricant (New or Used Oil) to which these ILs are added, the film thickness may vary, which then affects the friction performance of the whole tribo-system.

### 3.3. Wear Behavior

After the completion of each tribo-test, both the piston ring segment and the flat coupon samples showed smooth glossy worn areas depicting the polishing of the rough surface due to boundary lubrication conditions. Since the materials removed from the test samples were significant enough for comparison, therefore, wear volume measurements were carried out. Each case was evaluated by repeating the tests three times, and the mean of the measured wear volume was considered. Obtained mean values of wear volume were then used to calculate the specific wear rate using following formula [26]:

$$V = K \cdot F \cdot s \quad (1)$$

where  $V$  is the obtained wear volume,  $F$  is the applied load,  $s$  is the sliding distance, and  $K$  is the specific wear rate coefficient ( $\text{mm}^3/\text{Nm}$ ).

Table 4 clearly shows that Used Oil resulted in a higher wear volume of flat coupons than the New Oil. A plausible explanation for this effect is the depletion of protective film forming additives in Used Oil during its service in the actual engine prior to tribo-testing. In addition, the presence of wear debris in Used Oil, which is absent in New Oil, can accelerate the wear process by 2-body and/or 3-body abrasion mechanisms.

**Table 4.** Wear Volume and Specific Wear Rate results of flat coupons.

Flat Coupon Surface Lubricated with	Wear Volume, V (mm <sup>3</sup> )		Specific Wear Rate, K (×10 <sup>-7</sup> mm <sup>3</sup> /Nm)
	Mean	Std. Dev.	
New Oil	0.0095	0.0009	3.98
New Oil + 6% IL1	0.0085	0.0014	3.56
New Oil + 6% IL2	0.0121	0.0014	5.07
Used Oil	0.0217	0.0079	9.11
Used Oil + 6% IL1	0.0082	0.0001	3.45
Used Oil + 6% IL2	0.0077	0.0007	3.22

The effect of addition of ILs on the anti-wear performance of both New and Used oils can be seen in Table 4. Wear volume in the case of Used Oil has reduced by 62% and 64% by addition of IL1 and IL2, respectively. In addition, the mixtures of Used Oil with both ILs outperformed the fully formulated New Oil (with/without ILs). These observations indicate either the synergistic interaction between the remaining content of already present additives in Used Oil and the later-added ILs (as demonstrated by the authors for high temperature testing in the past [6]) or the stronger affinity of ILs to form films on surfaces than the existing additives.

The wear results for New Oil with IL1 show an improvement in performance, whereas a slight increase in wear is also observed after the addition of IL2. In the latter case, the antagonistic interaction between IL2 and already-existing additives in New Oil could have led to the generation of stresses responsible for a higher film removal rate than the film formation rate [6]. The wear results for all the cases of Used Oil are in line with the ECR curves (Figure 3), such that they follow a same trend as the boundary film thickness. The same comparison with ECR curves is not applicable in the case of New Oil.

The specific wear rates for cylinder liner materials in engine applications should be less than 10<sup>-7</sup> mm<sup>3</sup>/Nm [27]. Measured specific wear rate results for the flat coupons are noted to be in agreement with this suggested value. In addition, the wear rate results for the benchmark New Oil sample (with/without phosphonium ILs) are similar to those reported by other authors [9].

### 3.4. Wear Mechanisms

Due to the depletion of the anti-wear additives in Used Oil, severe plastic deformation of asperities on the flat coupons (Figure 5e) has taken place. However, the presence of such additives in fully formulated New Oil limited the plastic deformation of asperities (Figure 5a), such that some of the valleys of the ploughing grooves originated during the surface polishing (before tribo-testing) can still be observed. Unlike New Oil, wear lines generated by the debris present at the sliding interface, either as free particles leading to 3-body abrasion and/or embossed onto the counterpart piston ring running surface leading to 2-body abrasion, were also noted in the Used Oil case.

No significant change in the wearing mechanism is noted after the addition of ILs to the New Oil. However, the effect of the addition of IL1 (Figure 5f) and IL2 (Figure 5g) to the Used Oil is significantly beneficial, as the surface topographies in both cases are similar to that of fully formulated New Oil (Figure 5a). Clearly, the formation of a boundary film by ILs has reduced the effect of both plastic deformation and abrasive wear modes.

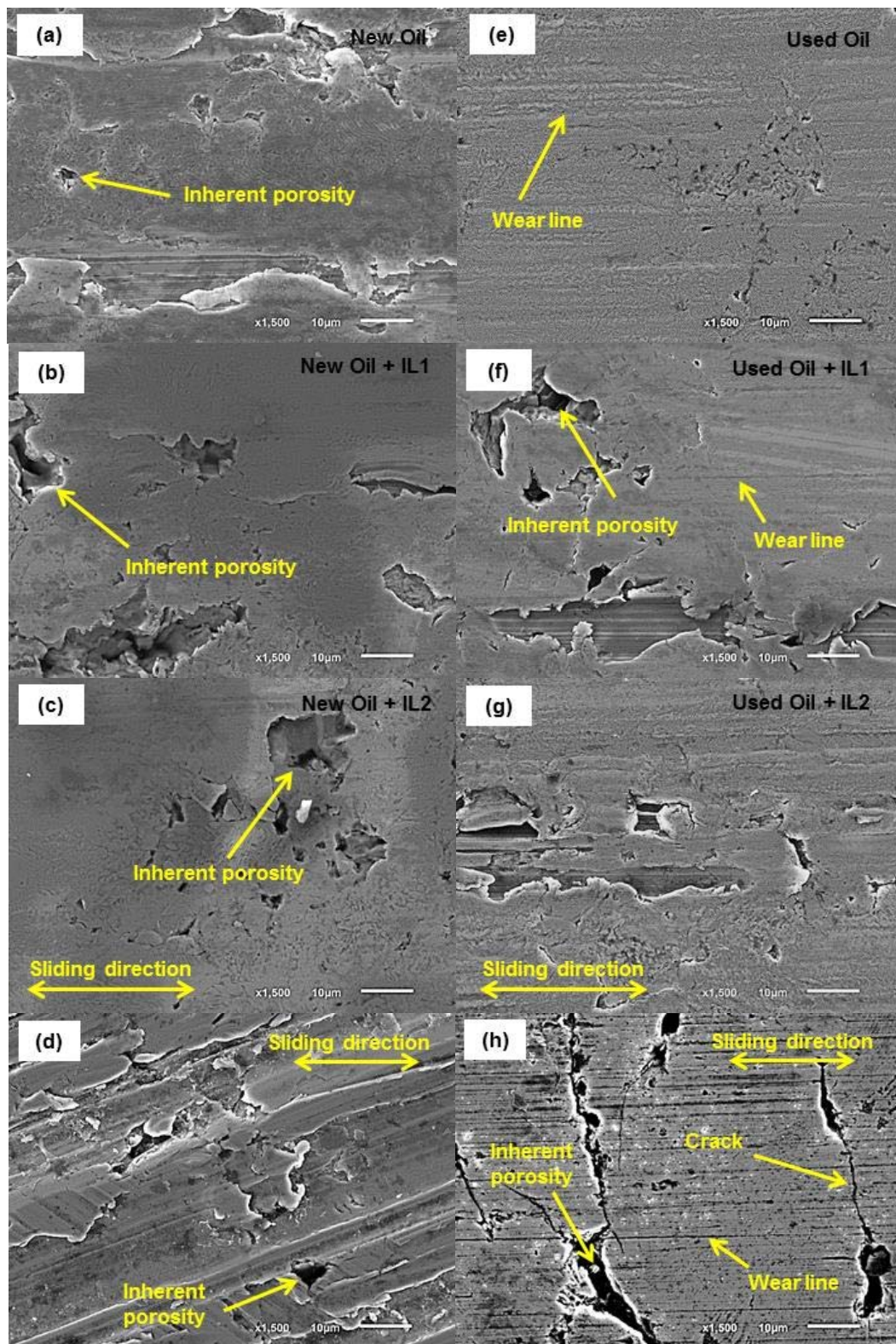


**Figure 5.** SEM images ( $\times 1500$ ) of flat coupons lubricated with New Oil (with/without ILs) in (a–c) and Used Oil (with/without ILs) in (e–g). SEM images ( $\times 1500$ ) of actual cylinder liner surface near TDC (d) unworn cross hatched surface of new liner; (h) worn surface of used liner at end of its service life.

In addition, the worn surface morphology of flat coupons (Figure 5a–c,e–g) was compared to that of the actual engine cylinder liners' bore surface near the TDC region (Figure 5d,h). For investigation, a new cylinder liner (Figure 5d) and a used cylinder liner at the end of its service life (Figure 5h) during the overhaul of an actual MAN D2840LE401 engine were obtained. Clearly, the crosshatch honing marks, which act as oil pockets on a new liner surface, have completely disappeared from the used liner surface that was at the end of its service life, leading to a very smooth surface finish. Similarly, the polishing marks are almost gone from the worn areas of flat coupons after 3 h of tribo-testing. Worn surfaces in both the actual liner and the flat coupons demonstrated abrasive wear lines in the direction of the sliding motion. Porous areas can also be seen in all cases, which are inherent to the cast iron material of the actual liner and coupons [9]. Surface cracks are only visible on the used liner surface. An explanation for this wear mechanism is the dynamic loading (variation of combustion gas pressure with piston stroke) experienced by the actual liner, leading to fatigue cracking of the surface [28]. This phenomenon is absent in flat coupons since these were subjected to constant static loading during the complete tribo-test duration (with little variation in contact pressure due to slight change in contact geometries). The similarities showed that the same basic wear mechanisms have taken place during the tribo-testing and in the real application. Therefore, it validates that the operating conditions experienced by the ring-liner configuration near the TDC region were adequately simulated at the bench level.

### 3.5. Chemical Analysis of Surface Films

Further information about the boundary film forming behavior of ILs was obtained by analyzing the chemical composition of surface films formed during the sliding process. The chemistry of engine-aged oil is complex and quite difficult to understand due to a number of chemical reactions taking place in lubricant during engine operation. However, an attempt is made to draw conclusions based on the available information. Table 5 shows no significant change in the concentrations of Ca, Zn, and P by the addition of ILs to the New Oil, whereas, those of C and O elements have greatly increased. On the contrary, the addition of ILs to Used Oil resulted in a slight increase in Ca and P elements, whereas there are reductions in Zn, C and O. Zn and P elements are present in ZDDP anti-wear additives and Ca is used typically as a detergent additive in diesel engine lubricants [2]. A plausible source of the C and O elements could be the long hydrocarbon chain structure of ILs containing oxygen atoms.

**Table 5.** Elemental concentration inside worn surface obtained by EDX analysis.

Flat Coupon Surface Lubricated with	Element Concentration (in wt. %)									
	C	O	Si	S	Ca	Zn	P	Mn	Fe	Cr
New Oil	8.41	3.88	2.37	0.30	0.36	0.34	0.26	0.71	83.27	0.10
New Oil + 6% IL1	19.44	5.17	2.01	0.11	0.34	0.31	0.22	nd	72.27	0.12
New Oil + 6% IL2	18.49	6.24	1.53	0.05	0.42	0.29	0.27	0.50	72.08	0.13
Used Oil	13.16	5.70	2.09	0.04	0.06	0.49	0.17	0.58	77.69	0.04
Used Oil + 6% IL1	10.22	4.30	2.28	0.12	0.19	nd	0.29	0.64	81.97	nd
Used Oil + 6% IL2	7.52	5.30	2.21	0.09	0.18	nd	0.30	0.65	83.78	nd

Nd—not detectable.

The above observations depict that the mixtures of New Oil and IL formed a boundary film composed of both the already-existing additives and the newly-added IL. On the other hand, the increase in P and reduction in Zn elements suggest the presence of a phosphonium-based IL and the absence, or very limited involvement, of ZDDP additives in the boundary film formed by Used Oil and IL mixtures. Therefore, the reactivity of ZDDP additives with the Fe-containing flat coupon seems to be suppressed by ILs. Such a behavior of ILs could be due to their strong affinity towards the metal surfaces to form a boundary film. The same is also true for ZDDP additives, which have a similar tendency. It could be explained on the basis that the engine-aged Used Oil has a depleted ZDDP content remaining to compete against IL to form film on the surface, therefore, the effect of ILs is likely to be stronger than the ZDDP additive. The higher concentration of the Zn element in Used Oil compared to New Oil before the addition of ILs is difficult to explain.

Furthermore, the presence of a Cr element in most cases suggests that a mild material transfer (adhesive wear) has taken place from the surface of chromium-coated piston ring (Table 2) to the flat coupon during the sliding process. Both ILs seem to eliminate this adhesive wear when added to the Used Oil.

Table 6 shows the chemical state of Fe elements within the wear scar region of flat coupons lubricated with the New and Used Oil with/without ILs. Clearly, Fe 2p peaks show that, in all cases, the Fe element (from flat coupon) is present in its oxidized state. However, since XPS analysis was performed on the surface, and only the first few nano-layers were examined, the boundary film may also contains Fe element in other chemical states in reaction with ILs and/or already existing additives, mainly near the interface between the flat coupon and the boundary film. Therefore, the depth profiling of the surface film using XPS could be useful to further investigate the presence of an Fe element. Due to limited resources in the current research, such an analysis is suggested for future research work.

**Table 6.** XPS results—binding energy shifts for Fe 2p<sub>3/2</sub> spectra.

Flat Coupon Surface Lubricated with	Binding Energy (eV)	Assigned Chemical Compounds	References
New Oil	708.8	Fe <sub>3</sub> O <sub>4</sub>	[29]
	710.6	Fe <sub>2</sub> O <sub>3</sub>	[30]
New Oil + 6% IL1	nd	-	-
New Oil + 6% IL2	708.4	Fe <sub>3</sub> O <sub>4</sub>	[31]
	710.2	Fe <sub>3</sub> O <sub>4</sub>	[31]
Used Oil	708.8	Fe <sub>3</sub> O <sub>4</sub>	[29]
	710.1	Fe <sub>3</sub> O <sub>4</sub>	[31]
Used Oil + 6% IL1	710.0	Fe <sub>3</sub> O <sub>4</sub>	[31]
Used Oil + 6% IL2	709.7	Fe <sub>3</sub> O <sub>4</sub>	[31]
	711.3	Fe <sub>2</sub> O <sub>3</sub>	[32–34]

Nd—not detectable.

Furthermore, Figure 6 shows the presence of Calcium Phosphate, Ca<sub>3</sub>(PO<sub>4</sub>)<sub>2</sub>, in the surface films formed by Used Oil, both with/without ILs. In addition, an increase in the intensity of the P2p band reflects the higher concentration of phosphorus after the addition of IL1 (Figure 6e) and IL2 (Figure 6f), compared to that of Used Oil without ILs (Figure 6d). These results also support the EDX observations mentioned in Table 5, and indicate the involvement of phosphorus-containing ILs in the process of boundary film formation.

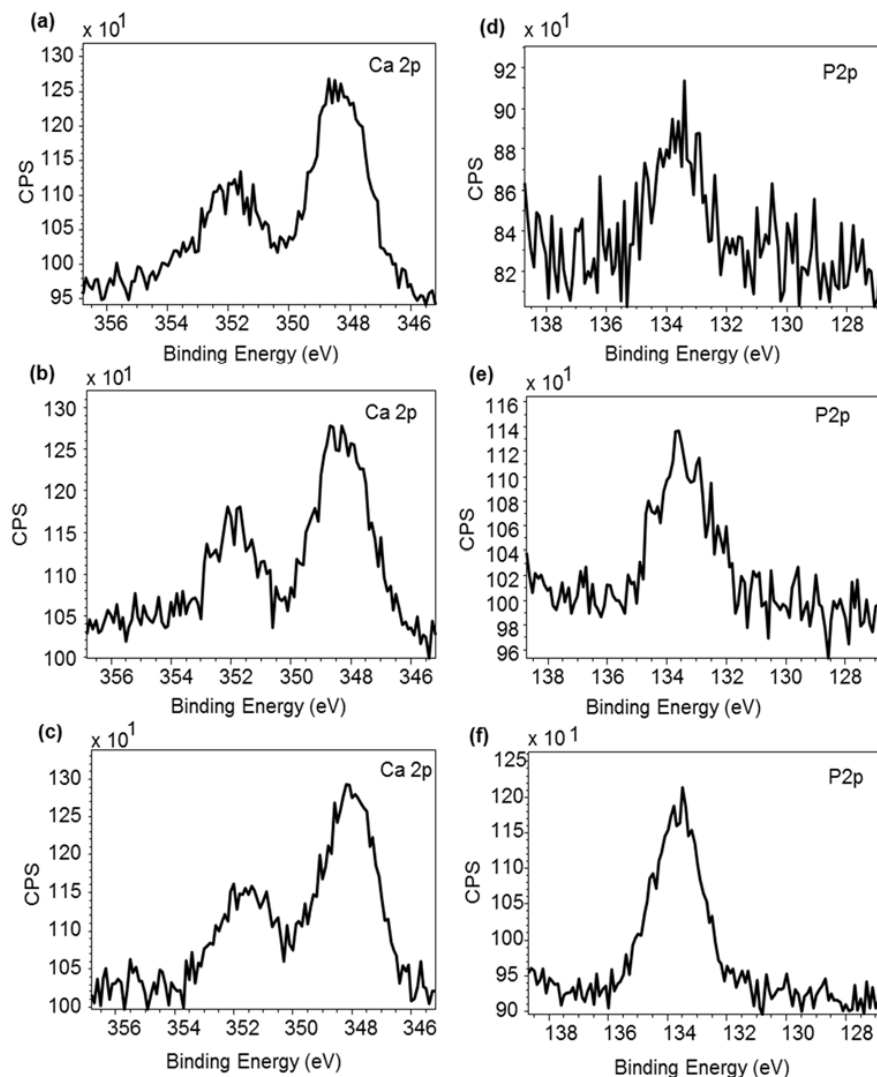


**Figure 6.** XPS spectra of Ca2p and P2p of flat coupons lubricated with Used Oil (a,d); Used Oil + 6% IL1 (b,c); Used Oil + 6% IL2 (c,f).

#### 4. Conclusions

From the results obtained the following conclusions can be drawn:

- The addition of phosphonium ILs to engine-aged lubricant results in a quicker initiation of the boundary film formation process, leading to a stable boundary film.
- Friction and wear performances of engine-aged lubricant outperformed fresh oil after the addition of both ILs.
- The formation of boundary film by ILs in engine-aged lubricant has reduced the effect of both plastic deformation and abrasive wear modes.
- Increase in concentration of phosphorus in boundary film formed by engine-aged lubricant and IL mixtures could suggest the involvement of phosphonium ILs in the boundary film formation process.

**Author Contributions:** Mayank Anand and Jose L. Viesca performed the experiments and surface analysis; Mayank Anand carried out the data analysis and wrote the paper with cooperation of Mark Hadfield, Jose L. Viesca and Antolin Hernández Battez; All authors were involved in the preparation and correction of the manuscript.

**Conflicts of Interest:** The authors declare no conflict of interest.

## References

1. Tung, S.C.; McMillan, M.L. Automotive tribology overview of current advances and challenges for the future. *Tribol. Int.* **2004**, *37*, 517–536.
2. Qu, J.; Blau, P.J.; Dai, S.; Luo, H.M.; Meyer, H.M. Ionic liquids as novel lubricants and additives for diesel engine applications. *Tribol. Lett.* **2009**, *35*, 181–189.
3. Mordukhovich, G.; Qu, J.; Howe, J.Y.; Bair, S.; Yu, B.; Luo, H.; Smolenski, D.J.; Blau, P.J.; Bunting, B.G.; Dai, S. A low-viscosity ionic liquid demonstrating superior lubricating performance from mixed to boundary lubrication. *Wear* **2013**, *301*, 740–746. [[CrossRef](#)]
4. Morris, N.; Rahmani, R.; Rahnejat, H.; King, P.; Fitzsimons, B. Tribology of piston compression ring conjunction under transient thermal mixed regime of lubrication. *Tribol. Int.* **2013**, *59*, 248–258. [[CrossRef](#)]
5. Mishra, P.; Balakrishnan, S.; Rahnejat, H. Tribology of compression ring-to-cylinder contact at reversal. *J. Eng. Tribol.* **2008**, *222*, 815–826. [[CrossRef](#)]
6. Anand, M.; Hadfield, M.; Viesca, J.L.; Thomas, B.; Hernández Battez, A.; Austen, S. Ionic liquids as tribological performance improving additive for in-service and used fully-formulated diesel engine lubricants. *Wear* **2015**, *334–335*, 67–74. [[CrossRef](#)]
7. Qu, J.; Truhan, J.J.; Dai, S.; Luo, H.; Blau, P.J. Ionic liquids with ammonium cations as lubricants or additives. *Tribol. Lett.* **2006**, *22*, 207–214. [[CrossRef](#)]
8. Mistry, K.; Fox, M.F.; Priest, M. Lubrication of an electroplated nickel matrix silicon carbide coated eutectic aluminium-silicon alloy automotive cylinder bore with an ionic liquid as a lubricant additive. *J. En. Tribol.* **2009**, *223*, 563–569. [[CrossRef](#)]
9. Yu, B.; Bansal, D.G.; Qu, J.; Sun, X.; Luo, H.; Dai, S.; Blau, P.J.; Bunting, B.G.; Mordukhovich, G.; Smolenski, D.J. Oil-miscible and non-corrosive phosphonium-based ionic liquids as candidate lubricant additives. *Wear* **2012**, *289*, 58–64. [[CrossRef](#)]
10. Qu, J.; Luo, H.; Chi, M.; Ma, C.; Blau, P.J.; Dai, S.; Viola, M.B. Comparison of an oil-miscible ionic liquid and ZDDP as a lubricant anti-wear additive. *Tribol. Int.* **2014**, *71*, 88–97. [[CrossRef](#)]
11. Predel, T.; Pohrer, B.; Schlücker, E. Ionic Liquids as alternative lubricants for special applications. *Chem. Eng. Technol.* **2010**, *33*, 132–136. [[CrossRef](#)]
12. Qu, J.; Blau, P.J.; Dai, S.; Luo, H.; Meyer, H.M., III; Truhan, J.J. Tribological characteristics of aluminum alloys sliding against steel lubricated by ammonium and imidazolium ionic liquids. *Wear* **2009**, *267*, 1226–1231. [[CrossRef](#)]
13. Young, W.C.; Budynas, R.G. Bodies in contact undergoing direct bearing and shear stress. In *Roark's Formulas for Stress and Strain*, 7th ed.; McGraw-Hill: New York, NY, USA, 2002; pp. 689–707.
14. Furey, M. Metallic contact and friction between sliding surfaces. *ASLE Trans.* **1961**, *4*, 1–11. [[CrossRef](#)]
15. Viesca, J.L.; Hernandez Battez, A.; González, R.; Reddyhoff, T.; Pérez, A.T.; Spikes, H.A. Assessing boundary film formation of lubricant additivated with 1-hexyl-3-methylimidazolium tetrafluoroborate using ECR as qualitative indicator. *Wear* **2010**, *269*, 112–117. [[CrossRef](#)]
16. Cambiella, A.; Benito, J.; Pazos, C.; Coca, J.; Ratoi, M.; Spikes, H.A. The effect of emulsifier concentration on the lubricating properties of oil-in-water emulsions. *Tribol. Lett.* **2006**, *22*, 53–65. [[CrossRef](#)]
17. Blanco, D.; Hernandez Battez, A.; Viesca, J.L.; González, R.; Fernández-González, A. Lubrication of CrN coating with ethyl-dimethyl-2-methoxyethylammonium tris (pentafluoroethyl) trifluorophosphate ionic liquid as additive to PAO 6. *Tribol. Lett.* **2011**, *41*, 295–302. [[CrossRef](#)]
18. Blanco, D.; González, R.; Hernández Battez, A.; Viesca, J.L.; Fernández-González, A. Use of ethyl-dimethyl-2-methoxyethylammonium tris (pentafluoroethyl) trifluorophosphate as base oil additive in the lubrication of TiN PVD coating. *Tribol. Int.* **2011**, *44*, 645–650. [[CrossRef](#)]
19. González, R.; Hernandez Battez, A.; Blanco, D.; Viesca, J.L.; Fernández-González, A. Lubrication of TiN, CrN and DLC PVD coatings with 1-butyl-1-methylpyrrolidinium tris (pentafluoroethyl) trifluorophosphate. *Tribol. Lett.* **2010**, *40*, 269–277. [[CrossRef](#)]
20. Hernandez Battez, A.; González, R.; Viesca, J.L.; Fernández-González, A.; Hadfield, M. Lubrication of PVD coatings with ethyl-dimethyl-2-methoxyethylammonium tris (pentafluoroethyl) trifluorophosphate. *Tribol. Int.* **2013**, *58*, 71–78. [[CrossRef](#)]

21. González, R.; Hernandez Battez, A.; Viesca, J.L.; Higuera-Garrido, A.; Fernández-González, A. Lubrication of DLC coatings with two tris(pentafluoroethyl)trifluorophosphate anion-based ionic liquids. *Tribol. Trans.* **2013**, *56*, 887–895. [[CrossRef](#)]
22. Viesca, J.L.; García, A.; Hernandez Battez, A.; González, R.; Monge, R.; Fernández-González, A.; Hadfield, M. FAP-anion ionic liquids used in the lubrication of a steel-steel contact. *Tribol. Lett.* **2013**, *52*, 431–437. [[CrossRef](#)]
23. Monge, R.; González, R.; Hernandez Battez, A.; Fernández-González, A.; Viesca, J.L.; García, A.; Hadfield, M. Ionic liquids as an additive in fully formulated wind turbine gearbox oils. *Wear* **2015**, *328–329*, 50–63. [[CrossRef](#)]
24. Yamaguchi, E.; Ryason, P.; Yeh, S.; Hansen, T. Boundary film formation by ZnDTPs and detergents using ECR. *Tribol. Trans.* **1998**, *41*, 262–272. [[CrossRef](#)]
25. Blau, P.J. *Friction Science and Technology: From Concepts to Applications*, 2nd ed.; CRC Press: Florida, FL, USA, 2012.
26. Greenall, A.; Neville, A.; Morina, A.; Sutton, M. Investigation of the interactions between a novel, organic anti-wear additive, ZDDP and overbased calcium sulphonate. *Tribol. Int.* **2012**, *46*, 52–61. [[CrossRef](#)]
27. Woydt, M.; Kelling, N. Testing the tribological properties of lubricants and materials for the system “piston ring/cylinder liner” outside of engines. *Ind. Lubr. Tribol.* **2003**, *55*, 213–222. [[CrossRef](#)]
28. Radil, K.C. *Test Method to Evaluate Cylinder Liner-Piston Ring Coatings for Advanced Heat Engines*; Memorandum Report ARL-MR-362; National Aeronautics and Space Administration Cleveland OH Lewis Research Center: Ohio, OH, USA, 1997.
29. Brainard, W.A.; Wheeler, D.R. An XPS study of the adherence of refractory carbide silicide and boride rf-sputtered wear-resistant coatings. *J. Vac. Sci. Technol.* **1978**, *15*, 1800–1805. [[CrossRef](#)]
30. Mathieu, H.J.; Landolt, D. An investigation of thin oxide films thermally grown *in situ* on Fe<sub>24</sub>Cr and Fe<sub>24</sub>Cr<sub>11</sub>Mo by auger electron spectroscopy and X-ray photoelectron spectroscopy. *Corros. Sci.* **1986**, *26*, 547–559. [[CrossRef](#)]
31. Tan, B.J.; Klabunde, K.J.; Sherwood, P.M. X-Ray photoelectron spectroscopy studies of solvated metal atom dispersed catalysts. Monometallic iron and bimetallic iron-cobalt particles on alumina. *Chem. Mater.* **1990**, *2*, 186–191. [[CrossRef](#)]
32. Wagner, C.; Riggs, W.; Davis, L.; Moulder, J.; Muilenberg, G. *Handbook of X-Ray Photoelectron Spectroscopy*; Perkin-Elmer: Eden Prairie, MN, USA, 1979.
33. Papparazzo, E. X-Ray photo-emission and Auger spectra of damage induced by Ar<sup>+</sup>-ion etching at SiO<sub>2</sub> surfaces. *J. Phys. D Appl. Phys.* **1987**, *20*. [[CrossRef](#)]
34. Seyama, H.; Soma, M. Fe 2p spectra of silicate minerals. *J. Electron. Spectrosc.* **1987**, *42*, 97–101. [[CrossRef](#)]



© 2016 by the authors; licensee MDPI, Basel, Switzerland. This article is an open access article distributed under the terms and conditions of the Creative Commons Attribution (CC-BY) license (<http://creativecommons.org/licenses/by/4.0/>).